Digestive and Liver Disease 51 (2019) 703–711

Contents lists available at ScienceDirect

Digestive and Liver Disease

journal homepage: www.elsevier.com/locate/dld

Liver, Pancreas and Biliary Tract

miRNA-448 inhibits cell growth by targeting BCL-2 in hepatocellular carcinoma

Zhi-bin Liao, Xiao-long Tan, Ke-shuai Dong, Hong-wei Zhang, Xiao-ping Chen, Liang Chu*, Bi-xiang Zhang*

Hepatic Surgery Center, Tongji Hospital, Tongji Medical College, Huazhong University of Science and Technology, Wuhan, Hubei, China

ARTICLE INFO

Article history:
Received 29 May 2018
Received in revised form
17 September 2018
Accepted 18 September 2018
Available online 28 September 2018

Keywords:
BCL-2
Hepatocellular carcinoma
miRNA-448
Tumor suppressor

ABSTRACT

Background: Increasing evidence indicates that aberrant micro (mi)RNA-448 expression plays a critical role in the progression of several human cancers. However, the function of miRNA-448 in hepatocellular carcinoma (HCC) has not been fully investigated.
Methods: miRNA-448 expression levels in HCC tissues, adjacent non-cancerous tissues (ANTs), and HCC cell lines were examined by quantitative real-time polymerase chain reaction (qRT-PCR). HCC cells were treated with a miRNA-448 mimic or inhibitor, followed by cell viability measurements with the CCK-8 assay. Venn diagram analysis predicted, and dual luciferase reporter assays verified, the target gene of miRNA-448. Expression of the target gene was detected by qRT-PCR and immunohistochemistry. Growth of miRNA-448- or target gene-expressing HCC xenograft tumors in nude mice was measured.
Results: miRNA-448 was expressed at a lower level in HCC tissues than ANTs, and correlated with a larger tumor size, incomplete tumor encapsulation, and advanced Barcelona Clinic Liver Cancer stage. miRNA-448 inhibited HCC cell growth. The downstream target of miRNA-448 was BCL-2, which was highly expressed in HCC tissues and its mRNA level was negatively correlated with miRNA-448 expression. *In vivo*, BCL-2 attenuated the tumor inhibiting effect of miRNA-448.
Conclusion: miRNA-448 functions as a tumor suppressor by targeting BCL-2 in HCC.

1. Introduction

Hepatocellular carcinoma (HCC) is one of the leading causes of cancer-related deaths worldwide, and its incidence is still increasing [1,2]. The Asia-Pacific area is the most prevalent region of HCC [3,4]. Many patients are first diagnosed at an advanced tumor stage. The five-year survival of HCC is low, and many patients die of cancer recurrence or metastasis. Therefore, it is critical to thoroughly understand HCC cancer biology and to seek new potential therapeutic approaches.

Micro (mi)RNAs are small regulatory RNAs that consist of about 22 nucleotides. Since the first report of miRNAs in 1980 [5], over 2500 miRNAs have been annotated in the human genome [6]. Mature miRNAs are localized to the RNA-induced silencing complex where they direct the complex to target mRNAs, leading to mRNA translational repression or degradation [7]. For example, miRNA-448 exerts a tumor suppressor role in numerous cancer types including breast [8–10], oral squamous cell [11], gastric [12], colorectal [13], and pancreatic ductal adenocarcinoma [14,15] cancers. However, the effects and precise mechanism of miRNA-448 in HCC are still elusive. The present study was designed to clarify the function of miRNA-448 and its downstream targets.

2. Materials and methods

2.1. Patients and tissue specimens

A total of 42 pairs of randomly selected snap-frozen tissues from patients who underwent hepatectomy at the Hepatic Surgery Center, Tongji Hospital of Huazhong University of Science and Technology (HUST) (Wuhan, China) from January 2010 to December 2012 were enrolled into this study. HCC diagnosis was confirmed by three types of clinical imaging (ultrasonography, computed tomography, or magnetic resonance imaging), together with a serum level

* Corresponding authors at: Hepatic Surgery Center, Tongji Hospital, Tongji Medical College, Huazhong University of Science and Technology, No.1095 Jie Fang Avenue, Wuhan, 430030, China.
E-mail addresses: liangchu@tjh.tjmu.edu.cn (L. Chu), bixiangzhang@163.com (B.-x. Zhang).

https://doi.org/10.1016/j.dld.2018.09.021
1590-8658/

of α-fetoprotein higher than 400 ng/mL. If diagnosis based on imaging and the α-fetoprotein level was uncertain, a needle biopsy was performed. Then, HCC was confirmed by histopathological examination of surgical samples. Two certified pathologists assessed the staining and scoring independently. They were blind to the patients' clinical and demographic information. If the staining score was identical between two pathologists, the score was adopted. If different staining scores were acquired from the two pathologists, the slide was reviewed by both pathologists and a final score was obtained.

Diagnosis of HCC is guided largely by disease stage, most often assessed using the Barcelona Clinic Liver Cancer staging system [16]. Surgery was indicated in an HCC patient with a liver tumor with sufficient residual liver volume, and lack of distant metastasis, decompensated cirrhosis, and organic dysfunction. All research on human materials was approved by the Ethics Committee of Tongji Hospital, HUST, and the study was conducted according to the Declaration of Helsinki principles. Written informed consent was obtained from each patient.

2.2. Cell lines and culture

MHCC97H cells were purchased from the Liver Cancer Institute of Fudan University (Shanghai, China). Huh7 and Hep3B cells were purchased from the China Center for Type Culture Collection (Wuhan, China). BEL7402 and HEK293T cells were deposited in the Hepatic Surgery Center, Tongji Hospital. All cell lines were cultured in Dulbecco's modified Eagle's medium (Gibco, Grand Island, NY, USA) supplemented with 10% fetal bovine serum (Gibco) and penicillin/streptomycin, and incubated in 5% CO_2 at 37 °C.

2.3. RNA isolation and the quantitative real-time polymerase chain reaction (qRT-PCR)

TRIzol reagent (Invitrogen, Carlsbad, CA, USA) was used to extract total RNA from tissues and cells according to the manufacturer's protocol. The reverse transcription of miRNA and mRNA was completed using reverse-transcription system (Toyobo, Osaka, Japan) and miRcute Plus miRNA First-Strand cDNA Synthesis (Tiangen, Beijing, China) kits. qPCR analysis for mRNA was performed with a standard SYBR Green PCR kit (Toyobo). The miRcute Plus miRNA qPCR Detection Kit (Tiangen) was used for miRNA according to the Step One system protocol (Applied Biosystems, Foster City, CA, USA). GAPDH and U6 were used as endogenous controls for the detection of mRNA and miRNA expression, respectively. Relative quantification analysis was performed using the comparative CT ($2^{-\Delta\Delta CT}$) method. Each experiment was repeated independently three times. Primer sequences were as follows: BCL-2 forward, 5′-GGTGGGGTCATGTGTGTGG-3′; BCL-2 reverse, 5′-CGGTTCAGGTACTCAGTCATCC-3′; miR-448, 5′-cgcTTGCATATGTAGGATGTCCCAT-3′.

2.4. Plasmid construction

The full length BCL-2 gene open reading frame was amplified by PCR and cloned into pCDNA3.1 to generate the pCDNA3.1-BCL-2 construct. pCDNA3.1 was used as the control.

2.5. Cell transfection and infection

All small RNA molecules were purchased from RiboBio (Guangzhou, China), including the miR-448 mimic, negative control mimic, miR-448 inhibitor, and negative control inhibitor. Cells were transiently transfected with the small RNA molecules or plasmids using the riboFect™ CP Transfection Kit (333T) (Invitrogen) according to the manufacturer's protocol. Cells were infected with lentivirus containing the full length BCL-2 CDS domain to generate cells stably overexpressing BCL-2.

2.6. Cell proliferation assay

BEL7402 and Huh7 cells were transfected with the miR-448 mimic, inhibitor, or scramble 24 h before seeding into 96-well plates at 1000 cells/well. The Cell Counting Kit-8 (CCK-8, Dojindo, Kumamoto, Japan) reagent was added to the wells, and absorbance values in each well were measured with a microplate reader at 450 nM. All experiments were performed three times and average absorbance values are shown.

2.7. Luciferase assay

The entire 3′-untranslated region (UTR) of the BCL-2 gene was cloned into the psiCHECK™-2-vector (Promega, Madison, WI, USA) at a site immediately downstream of the Renilla luciferase gene. Three mutations in the 3′-UTR (Mut 1, Mut 2, and Mut 1.2) were generated with the QuickChange Site-Directed Mutagenesis kit (Stratagene, La Jolla, CA, USA). About 1×10^5 BEL-7402 cells/well were seeded into 24-well plates for 24 h before transfection. Cells were co-transfected with 50 ng of the psiCHECK™-2-vector, and 50 nM of the miR-448 or scrambled mimic using Lipofectamine 2000 (Invitrogen). Cell lysates were prepared using Passive Lysis Buffer (Promega) 48 h after transfection, and luciferase activity was measured using the Dual-Luciferase Reporter Assay (Promega). Experiments were repeated three times.

2.8. Western blot analysis

Protein concentrations were determined with a BCA Protein Assay Kit (Bio-Rad, Hercules, CA, USA) and equal amounts of protein were analyzed by SDS-PAGE. Gels were electroblotted onto nitrocellulose membranes (EMD Millipore, Billerica, MA, USA). After blocking with 5% non-fat milk in Tris-buffered saline containing 0.1% Tween-20 for 2 h, membranes were incubated at 4 °C overnight with the primary antibodies (BCL-2 and GAPDH; Cell Signaling Technology, Danvers, MA, USA). Then, membranes were incubated with horseradish peroxidase-conjugated secondary antibodies and detected by an enhanced chemiluminescence system (EMD Millipore). The experiment was repeated three times.

2.9. Immunohistochemical staining and the terminal deoxynucleotidyl transferase dUTP nick-end labeling (TUNEL) assay

Formalin fixed, paraffin-embedded sections were deparaffinized in xylene and rehydrated through graded concentrations of ethanol. Microwave heating in a 10 mM Tris-base-1 mM EDTA solution (pH 9.0) was used to retrieve antigens. Endogenous peroxidases were blocked with 3% H_2O_2 in methanol. Sections were incubated with 1:100 BCL-2 (EMD Millipore) or 1:200 proliferating cell nuclear antigen (PCNA) (Cell Signaling Technology) primary antibodies at 4 °C overnight. Incubation with the secondary antibody and detection of peroxidase activity was achieved by using the EnVision kit (Dako, Glostrup, Denmark). Hematoxylin (Sigma-Aldrich, St. Louis, MO, USA) was used to counterstain the nucleus. Immunohistochemistry scores were obtained by multiplying the percentage of positive staining score to the intensity score as described previously [17]. Overall scores of >6 and ≤6 were defined as high and low expression, respectively. The TUNEL assay was performed using the In Situ Cell Death Detection Kit (BD Biosciences, Franklin Lakes, NJ, USA) according to the manufacturer's instructions.

2.10. Xenograft tumor model

The animal study was approved by the Ethics Committee of Tongji Hospital, HUST. Briefly, 4–5-week-old male nude mice were purchased from HFK BioScience (Beijing, China) and maintained in specific-pathogen-free conditions. BEL7402 and BEL7402-BCL-2 cells (1×10^6) were suspended in 100 μL Dulbecco's modified Eagle's medium and injected subcutaneously into nude mice. One week after cell inoculation, miRNA-448 or scrambled mimics were injected into the tumors. All mice were routinely monitored, and sacrificed at day 30 of inoculation. Tumor volumes were calculated according to the following equation: V (volume, mm^3) = 0.5 × L (length, mm) × W^2 (width, mm^2) [18].

2.11. Statistical analyses

Statistical analyses were performed by SPSS 19.0 (IBM, Chicago, IL, USA) or Prism 6.0 (GraphPad Software, La Jolla, CA, USA) software. Quantitative data were compared by a two-tailed Student's t-test, analysis of variance with the Bonferroni post-hoc test, or a nonparametric test such as the Wilcoxon signed-rank test. A value of $p < 0.05$ was considered statistically significant.

3. Results

3.1. miRNA-448 is downregulated in HCC tissues

To evaluate the clinical significance of miRNA-448 in HCC, we detected its expression pattern in 42 pairs of HCC tissue and adjacent non-cancerous tissue (ANT) by the qRT-PCR. The results showed that the miRNA-448 level was significantly higher in ANT compared to HCC tissue (Fig. 1A, B). Clinicopathological data showed that downregulation of miRNA-448 correlated with larger tumor size ($p = 0.019$), incomplete tumor encapsulation ($p = 0.020$), and advanced Barcelona Clinic Liver Cancer stage ($p = 0.037$) (Table 1). We then detected miRNA-448 expression in four HCC cell lines: BEL7402, MHCC97H, Hep3B, and Huh7. BEL7402 and MHCC97H cells [19,20] possess higher proliferation and metastasis potentials than Hep3B and Huh7 cells [21–23]. The expression of miRNA-448 was much lower in BEL7402 and MHCC97H cells than in Hep3B and Huh7 cells (Fig. 1C).

Table 1
Correlation between miRNA-448 expression and clinicopathologic characteristics in 42 HCC patients.

Clinicopathologic variables	Low expression	High expression	P value
Gender			
Male	11	27	
Female	1	3	0.680
Age			
≤50	5	19	
>50	7	11	0.174
AFP (ug/L)			
≤20	2	9	
>20	10	21	0.318
GGT(u/l)			
≤54	3	16	
>54	9	14	0.092
ALT(ng/ml)			
≤75	12	26	
>75	0	4	0.245
HBV			
Negative	4	3	
Positive	8	27	0.088
Cirrhosis			
No	5	9	
Yes	7	21	0.353
Tumor size (cm)			
≤5	1	14	
>5	11	16	**0.019**[a]
Tumor encapsulation			
Complete	4	22	
Incomplete	8	8	**0.020**[a]
Tumor number			
Single	10	25	
Multiple	2	5	0.660
Vascular invasion			
No	9	24	
Yes	3	6	0.509
Differentiation			
I–II	4	11	
III–IV	8	19	0.566
BCLC stage			
0 + A	5	23	
B + C	7	7	**0.037**[a]

[a] The values had statistically significant differences.

3.2. miRNA-448 inhibits HCC cell proliferation

To investigate the effect of miRNA-448 on cell proliferation, we enhanced its expression by a miRNA-448 mimic in BEL7402 and MHCC97H cells. The CCK-8 assay showed that miRNA-448 overexpression inhibited cell proliferation compared to control cells (Fig. 2A, B). Downregulation of miRNA-448 by an inhibitor promoted Huh7 cell proliferation (Fig. 2C, D).

3.3. BCL-2 is the downstream target of miRNA-448

Venn diagram analysis of predicted miRNA-448 targets was performed from four independent databases: miRDB [24,25], miRWalk [26,27], microT-CDS [28,29], and TargetScan [30]. This analysis revealed four candidate targets of miRNA-448: BCL-2, ZBTB34, GAN, and C11orf87 (Fig. 3A). Manipulation of miRNA-448 expression in Hep3 B and MHCC97H cells affected BCL-2 mRNA levels (Fig. 3B).

To validate that BCL-2 was a direct target of miRNA-448, potential binding sites in the BCL-2 3′-UTR were identified (Fig. 3C) and a dual luciferase reporter assay was performed. Reporter vectors containing wild-type or mutated binding sequences were transfected into HEK293T cells along with miRNA-448 or scrambled mimics. The results showed that co-transfection of BCL-2-wild-type, BCL-2-MUT2, and the miRNA-448 mimic led to a significant increase in luciferase activity compared to the control group, whereas co-transfection of BCL-2-MUT1, BCL-2-MUT1.2, and the miRNA-448 mimic had no effect (Fig. 3D). This suggested that MUT1 and MUT1.2 abolished the binding activity of miRNA-448 to BCL-2.

To confirm the functional significance of miRNA-448 on BCL-2, we overexpressed miRNA-448 in BEL7402 cells using various quantities of the miRNA-448 mimic. The mRNA and protein levels of BCL-2 decreased coordinately with increasing doses of the miRNA-448 mimic (Fig. 3E, F). Moreover, overexpression and downregulation of miRNA-448 in HCC cell lines yielded consistent results (Fig. 3G, H).

3.4. BCL-2 is negatively correlated with miRNA-448 in HCC tissues

We assessed the correlation between miRNA-448 and BCL-2 in clinical tissue samples. qRT-PCR detection of BCL-2 mRNA was carried out in the same 42 pairs of tissues previously analyzed for miRNA-448 (Fig. 1A, B). The results showed that BCL-2 mRNA was significantly upregulated in HCC tissues compared with ANTs (Fig. 4A), and the level of BCL-2 mRNA was negatively correlated

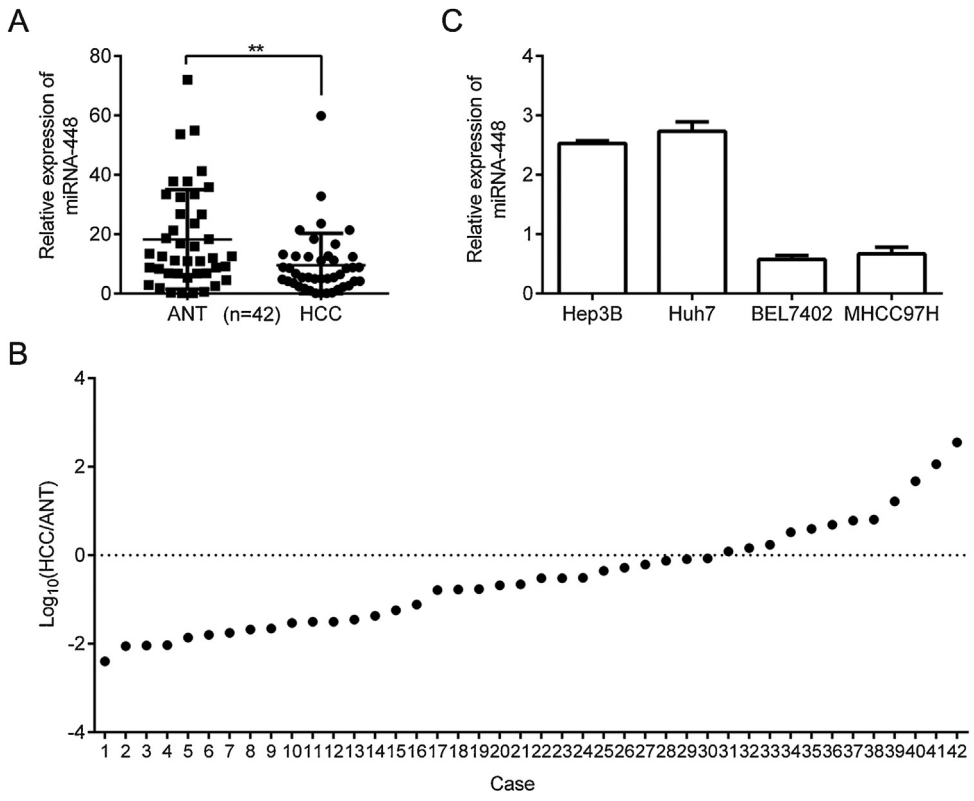

Fig. 1. Expression of miRNA-448 in hepatocellular carcinoma (HCC).
(A) miRNA-448 levels in paired HCC tissues and adjacent non-cancerous tissues (ANTs) as measured by the quantitative real-time polymerase chain reaction. Results are shown as means ± S.D. (n = 42). (B) Comparison of miRNA-448 expression in HCC tissues and ANTs. The y-axis is the log10 of fold-change (n = 42). (C) Expression of miRNA-448 in four HCC cell lines. Bars represent means ± S.D. **p < 0.01.

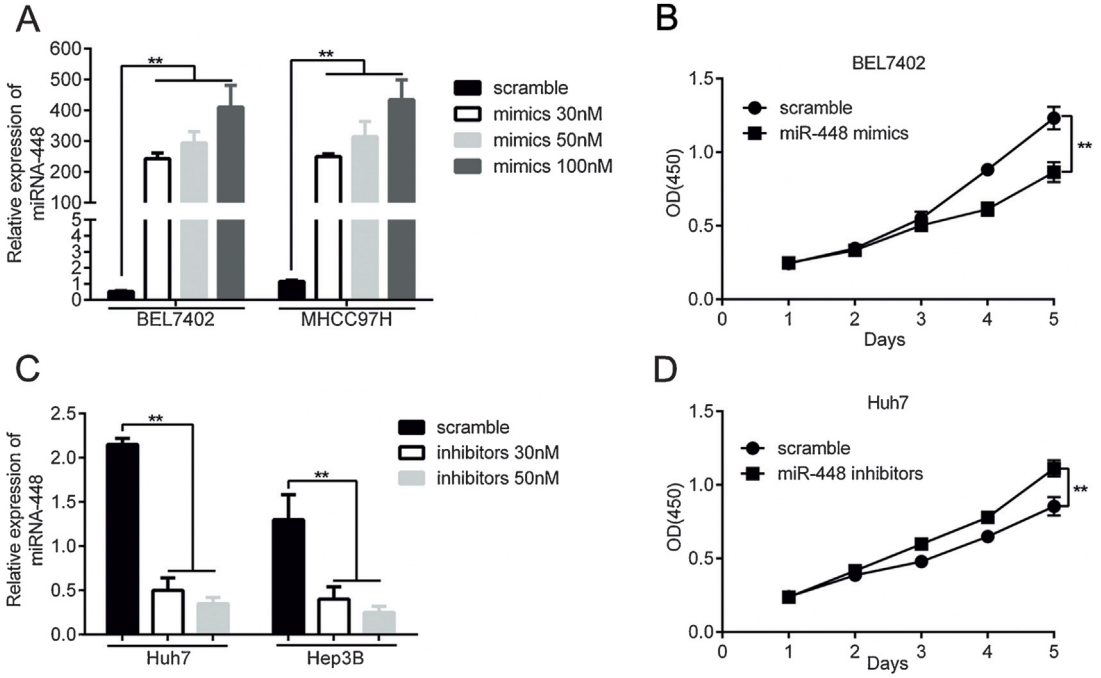

Fig. 2. miRNA-448 inhibits cell proliferation.
(A, C) Overexpression and downregulation of miRNA-448 in hepatocellular carcinoma (HCC) cells using a miRNA-448 mimic (A) or inhibitor (C), respectively, as measured by the quantitative real-time polymerase chain reaction. (B) miRNA-448 overexpression in BEL7402 cells inhibits cell proliferation as measured by the CCK8 assay. (D) Downregulation of miRNA-448 in Huh7 cells promotes cell proliferation as measured by the CCK8 assay. **p < 0.01.

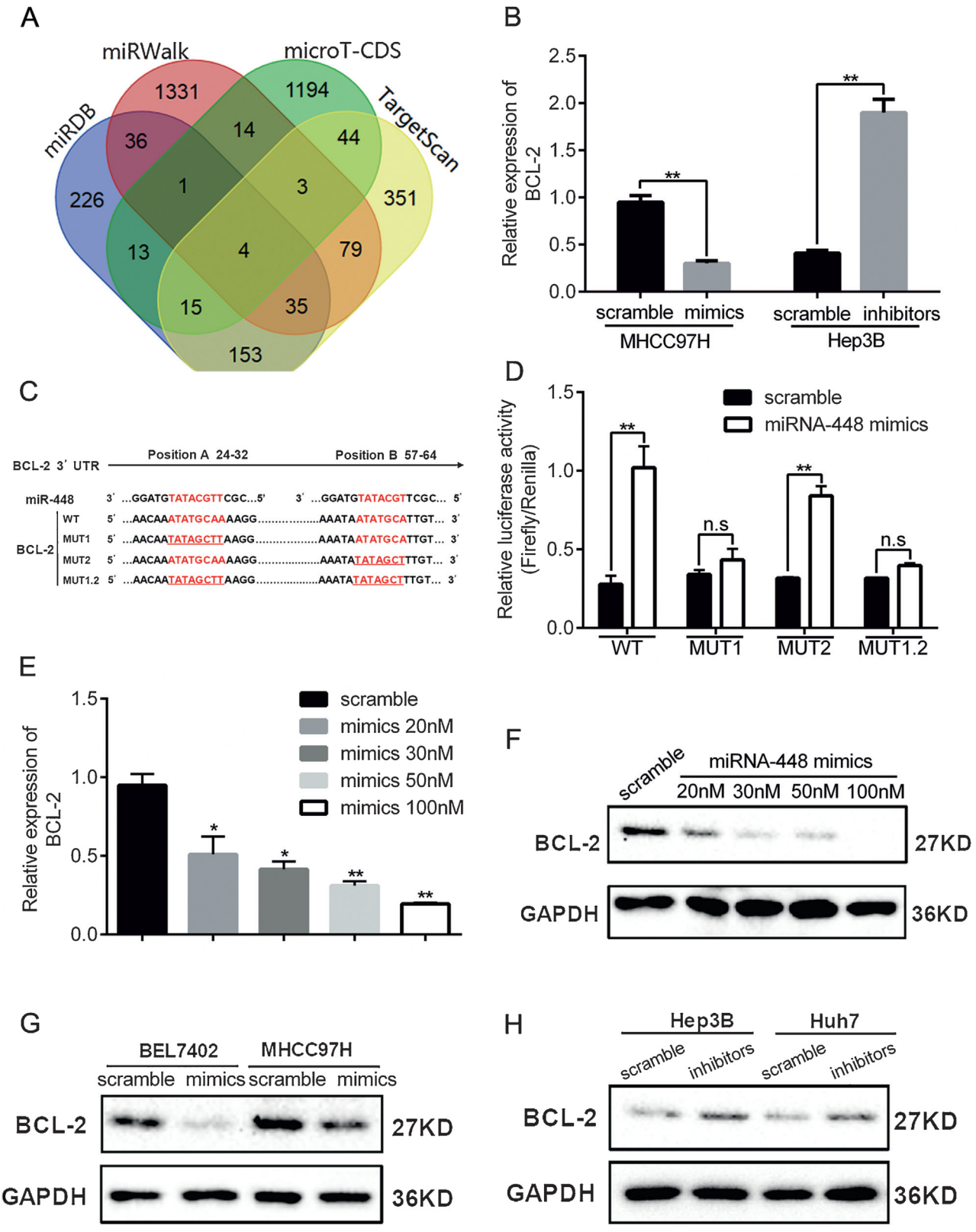

Fig. 3. BCL-2 is the target of miRNA-448.
(A) Venn diagram analyses of four independent databases reveals four possible targets of miRNA-448. (B) Overexpression and downregulation of miRNA-448 in MHCC97H and Hep3B cells changes the BCL-2 mRNA level as measured by the quantitative real-time polymerase chain reaction. (C) Potential miRNA-448 binding sites in the BCL-2 3′-untranslated region (UTR) and three mutated constructs. (D) Wild-type (WT) or mutated BCL-2 3′-UTR luciferase reporter plasmids were co-transfected with miRNA-448 or scrambled mimics into HEK293T cells. MUT1 and MUT1.2 abolish the binding activity of miRNA-448 to the BCL-2 3′-UTR. (E, F) Enhanced miRNA-448 expression in BEL7402 cells suppresses BCL-2 mRNA (E) and protein (F) levels in a dose-dependent manner. (G, H) Manipulation of miRNA-448 in four HCC cell lines correspondingly changes BCL-2 protein expression. *$p < 0.05$. **$p < 0.01$. n.s, non-significant.

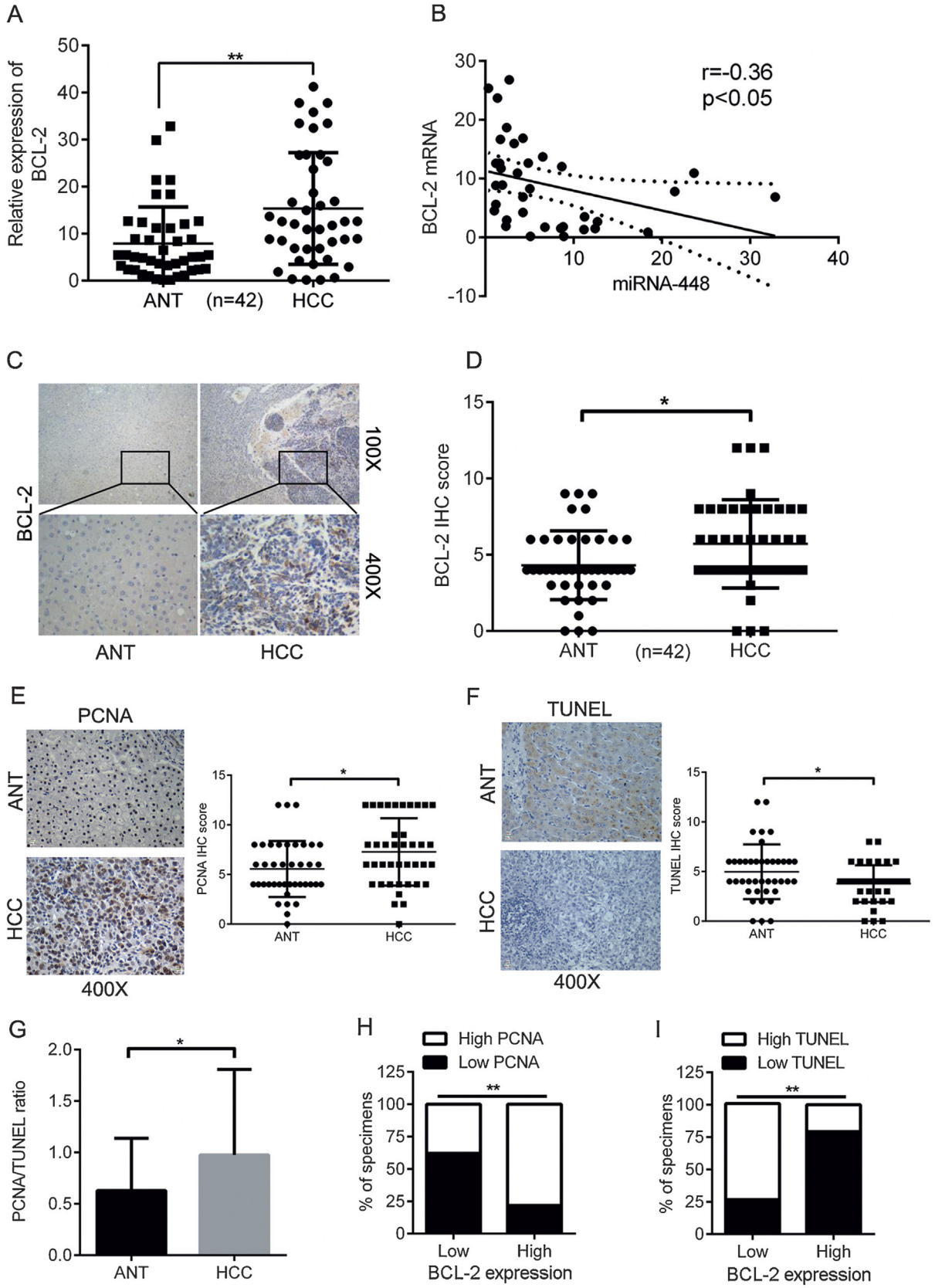

Fig. 4. Expression of BCL-2 in hepatocellular carcinoma (HCC).
(A) Quantitative real-time polymerase chain reaction analyses of BCL-2 mRNA in paired HCC tissue and adjacent non-cancerous tissue (ANT). Results are shown as means ± S.D. (n = 42). (B) Linear regression analysis between BCL-2 mRNA and miRNA-448 ($r = -0.36$, $p < 0.05$). (C) Representative images of BCL-2 staining in 42 pairs of HCC tissues and ANTs. (D) Statistical analysis of BCL-2 scoring shows the upregulation of BCL-2 in HCC tissues. (E) Representative immunohistochemistry images and quantitation of proliferating cell nuclear antigen (PCNA). (F) Representative terminal deoxynucleotidyl transferase dUTP nick-end labeling (TUNEL) images and quantitation of staining. E and F utilized 42 pairs of HCC tissues and ANTs. (G) Statistical analysis of the PCNA/TUNEL ratio in ANTs and HCC tissues. (H, I) The histogram displays the percentages of specimens showing low or high BCL-2 expression in relation to the expression levels of PCNA (H) or the extent of apoptosis by the TUNEL assay (I). *$p < 0.05$, **$p < 0.01$.

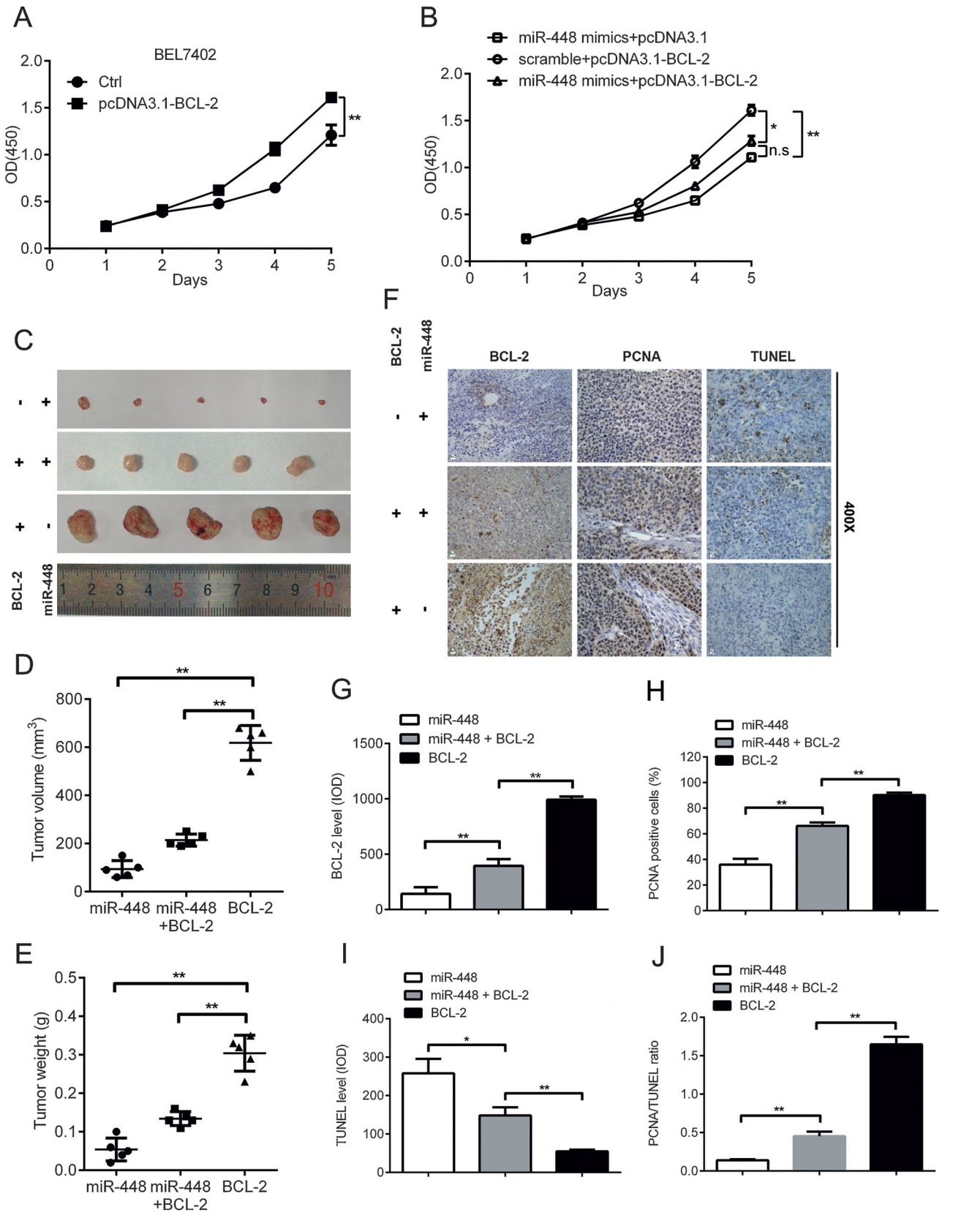

Fig. 5. BCL-2 attenuates the growth inhibition effect of miRNA-448.
Transfection of pcDNA3.1-BCL-2 into BEL7402 cells promotes cell proliferation as measured by the CCK8 assay. (B) Overexpression of miRNA-448 in BEL7402 cells overexpressing BCL-2 decreases cell proliferation. (C) Images of isolated xenograft BEL7402 cell tumors in the miRNA-448 group (first row), BCL-2 and miRNA-448 co-expression group (second row), and BCL-2 group (third row). (D) Tumor xenograft volumes are reduced by overexpressing miRNA-448. (E) Tumor xenograft weights are reduced by overexpressing miRNA-448. (F) Representative immunohistochemistry images of BCL-2 and proliferating cell nuclear antigen (PCNA), and terminal deoxynucleotidyl transferase dUTP nick-end labeling (TUNEL) staining in tumor tissues of subcutaneous xenografts. (G–I) Quantification of BCL-2 (G), PCNA (H), and TUNEL (I) staining in (F). (J) Statistical analysis of the PCNA/TUNEL ratio in (F). *$p < 0.05$, **$p < 0.01$. IOD, integrated optical density.

with miRNA-448 ($r = -0.36$, $p < 0.05$) (Fig. 4B). Immunohistochemistry staining of BCL-2 in the 42 pairs of HCC tissues and ANTs showed that BCL-2 expression in HCC tissues was significantly higher than that in ANTs (Fig. 4C, D). HCC tissues displayed higher cell proliferation and lower cell apoptosis than ANTs (Fig. 4E, F). The PCNA/TUNEL ratio was higher in HCC tissues (Fig. 4G), and the expression of PCNA was strong in 18 of 23 HCC specimens expressing high levels of BCL-2 (Fig. 4H). Concurrently, an inverse pattern of TUNEL staining was found in the same patient cohort (Fig. 4I).

3.5. *BCL-2 partially directs the tumor inhibitory function of miRNA-448*

Transfection of pcDNA3.1-BCL-2 into BEL7402 cells promoted cell proliferation (Fig. 5A), and overexpression of miRNA-448 attenuated this growth promoting effect (Fig. 5B). BEL7402 mock transfected cells, and BEL7402 cells with BCL-2 stable overexpression mediated by lentivirus, were injected subcutaneously into nude mice. One week later, the tumors were injected with miRNA-448 or scrambled mimics. Thirty days after tumor cell inoculation, the tumor volume and weight were noticeably decreased in the miRNA-448 and BCL-2 combination group compared with the BCL-2 control group (Fig. 5C–E). Moreover, cell proliferation decreased, and apoptosis increased in the miRNA-448 and BCL-2 combination group compared with the BCL-2 control group (Fig. 5F–J). Taken together, these results demonstrated that miRNA-448 suppressed BCL-2-enhanced BEL7402 tumor growth.

4. Discussion

In this study, we showed that miRNA-448 was downregulated in HCC tissues and that low expression of miRNA-448 correlated with several malignant clinical features (Fig. 1A, B and Table 1). The expression of miRNA-448 was lower in more malignant HCC cell lines (Fig. 1C). Manipulation of miRNA-448 expression in HCC cells validated its growth inhibition effect (Fig. 2).

By analyzing online bioinformatics data, BCL-2 was identified as a potential target of miRNA-448. The dual luciferase reporter assay validated BCL-2 as a target, and miRNA-448 regulated its expression (Fig. 3). The mRNA and protein levels of BCL-2 were upregulated in HCC tissues, and there was a negative correlation between BCL-2 mRNA and miRNA-448 in HCC tissues (Fig. 4). Functional validation studies showed that enhancing miRNA-448 expression inhibited cell proliferation and tumor growth, and overexpression of BCL-2 attenuated this effect both in cells and in xenograft tumors (Fig. 5).

BCL-2 in involved in apoptosis, a programmed form of cell death that is induced under various stress conditions, is essential for the development and function of multicellular systems [31,32]. Evading cell apoptosis is a key hallmark of cancers [33], and BCL-2 plays a pivotal role in this process. BCL-2 is an integral mitochondrial membrane protein that blocks the apoptosis process by interacting with and antagonizing pro-apoptotic BCL-2 family members [34,35].

BCL-2 was first identified as an oncogene in B-cell malignancies [36]. Later, it was reported in prostate [37,38] and breast [39,40] cancers as a proto-oncogene. Several possible therapeutic agents have been developed targeting different BCL-2 domains. ABT-737 and ABT-263 bind to the hydrophobic pocket of BCL-2 with high affinity and subsequently disrupt its anti-apoptotic function [41]. A tethered indole was incorporated into ABT-263 to fill the P4 hot spot to generate a more selective BCL-2 inhibitor that interacted specifically with aspartic acid (Asp 103) of BCL-2, resulting in the BCL-2-selective inhibitor, ABT-199 [42]. The BH4 domain of BCL-2 is the docking site for screening of potential therapeutic targets because it is critical for the anti-apoptotic function of BCL-2. BDA-366 is a specific target of the BH4 domain and converts BCL-2 from a survival to a cell death inducing molecule through a conformational change [43,44].

MicroRNAs are single-stranded non-coding RNA molecules. The length of miRNAs is about 22 nucleotides. miRNAs have been extensively regarded as controllers in biological processes and are closely related with tumorigenesis. Our findings suggest that miRNA-448 could be a novel therapeutic target to alter BCL-2 function. miRNAs usually regulate gene expression at the post-transcriptional level by binding complimentary sequences in the target mRNA 3′-UTR [45]. They can function as tumor suppressors by negatively modulating their mRNA targets [46]. miRNA-448 suppresses tumor growth in colorectal and gastric cancer [13], inhibits cancer proliferation in oral squamous cell carcinoma [11], and suppresses bladder cancer cell growth and proliferation [47]. Zhu et al. [48] reported that low expression of miRNA-448 induced the epithelial-to-mesenchymal transition by partially regulating Rho-associated coiled-coil-containing protein kinase 2 in HCC.

In conclusion, because of the lack of efficient chemotherapy for treating HCC, the findings reported in this study, and other reports, suggest that miRNA-448 and BCL-2 may be promising targets in the future development of HCC treatments.

Conflict of interest

None declared.

Acknowledgments

We thank Lanping Ding (Institute of Organ Transplantation, Tongji Hospital) and Shunchang Zhou (Department of Experimental Zoology, Tongji Medical College) for animal care, and Wei Dong (Hepatic Surgery Center, Tongji Hospital) for insightful discussions. This work was supported by National Natural Science Fund (31671348, 81572427, 81572855) and Graduates' Innovation Fund, Huazhong University of Science and Technology (5003540055).

References

[1] Miller KD, Siegel RL, Lin CC, Mariotto AB, Kramer JL, Rowland JH, et al. Cancer treatment and survivorship statistics, 2016. CA Cancer J Clin 2016;66:271–89.
[2] Siegel RL, Miller KD, Jemal A. Cancer statistics, 2016. CA Cancer J Clin 2016;66:7–30.
[3] Ferlay J, Soerjomataram I, Dikshit R, Eser S, Mathers C, Rebelo M, et al. Cancer incidence and mortality worldwide: sources, methods and major patterns in GLOBOCAN 2012. Int J Cancer 2015;136:E359–86.
[4] Torre LA, Bray F, Siegel RL, Ferlay J, Lortet-Tieulent J, Jemal A. Global cancer statistics, 2012. CA Cancer J Clin 2015;65:87–108.
[5] Horvitz HR, Sulston JE. Isolation and genetic characterization of cell-lineage mutants of the nematode *Caenorhabditis elegans*. Genetics 1980;96:435–54.
[6] Griffiths-Jones S, Grocock RJ, van Dongen S, Bateman A, Enright AJ. miRBase: microRNA sequences, targets and gene nomenclature. Nucleic Acids Res 2006;34:D140–4.
[7] Hammond SM. An overview of microRNAs. Adv Drug Deliv Rev 2015;87:3–14.
[8] Bamodu OA, Huang WC, Lee WH, Wu A, Wang LS, Hsiao M, et al. Aberrant KDM5B expression promotes aggressive breast cancer through MALAT1 overexpression and downregulation of hsa-miR-448. BMC Cancer 2016;16:160.
[9] Jiang X, Zhou Y, Sun AJ, Xue JL. NEAT1 contributes to breast cancer progression through modulating miR-448 and ZEB1. J Cell Physiol 2018, http://dx.doi.org/10.1002/jcp.26470 [ahead of print].
[10] Ma P, Ni K, Ke J, Zhang W, Feng Y, Mao Q. miR-448 inhibits the epithelial-mesenchymal transition in breast cancer cells by directly targeting the E-cadherin repressor ZEB1/2. Exp Biol Med 2018;243:473–80.
[11] Shen L, Liu L, Ge L, Xie L, Liu S, Sang L, et al. miR-448 downregulates MPPED2 to promote cancer proliferation and inhibit apoptosis in oral squamous cell carcinoma. Exp Therap Med 2016;12:2747–52.
[12] Wu X, Tang H, Liu G, Wang H, Shu J, Sun F. miR-448 suppressed gastric cancer proliferation and invasion by regulating ADAM10. Tumour Biol 2016;37:10545–51.
[13] Li B, Ge L, Li M, Wang L, Li Z. miR-448 suppresses proliferation and invasion by regulating IGF1R in colorectal cancer cells. Am J Transl Res 2016;8:3013–22.
[14] Yu DL, Zhang T, Wu K, Li Y, Wang J, Chen J, et al. MicroRNA-448 suppresses metastasis of pancreatic ductal adenocarcinoma through targeting JAK1/STAT3 pathway. Oncol Rep 2017;38:1075–82.

[15] Zhao L, Kong H, Sun H, Chen Z, Chen B, Zhou M. LncRNA-PVT1 promotes pancreatic cancer cells proliferation and migration through acting as a molecular sponge to regulate miR-448. J Cell Physiol 2018;233:4044–55.
[16] European Association For The Study Of The Liver, European Organisation For Research And Treatment Of Cancer. EASL-EORTC clinical practice guidelines: management of hepatocellular carcinoma. J Hepatol 2012;56:908–43.
[17] Li JC, Yang XR, Sun HX, Xu Y, Zhou J, Qiu SJ, et al. Up-regulation of Kruppel-like factor 8 promotes tumor invasion and indicates poor prognosis for hepatocellular carcinoma. Gastroenterology 2010;139:2146–57, e12.
[18] Zhang B, Halder SK, Kashikar ND, Cho YJ, Datta A, Gorden DL, et al. Antimetastatic role of Smad4 signaling in colorectal cancer. Gastroenterology 2010;138:969–80, e1–3.
[19] Ding ZY, Jin GN, Wang W, Chen WX, Wu YH, Ai X, et al. Reduced expression of transcriptional intermediary factor 1 gamma promotes metastasis and indicates poor prognosis of hepatocellular carcinoma. Hepatology 2014;60:1620–36.
[20] Tang ZY, Ye SL, Liu YK, Qin LX, Sun HC, Ye QH, et al. A decade's studies on metastasis of hepatocellular carcinoma. J Cancer Res Clin Oncol 2004;130:187–96.
[21] Giannelli G, Fransvea E, Marinosci F, Bergamini C, Colucci S, Schiraldi O, et al. Transforming growth factor-beta1 triggers hepatocellular carcinoma invasiveness via alpha3beta1 integrin. Am J Pathol 2002;161:183–93.
[22] Lee JS, Thorgeirsson SS. Functional and genomic implications of global gene expression profiles in cell lines from human hepatocellular cancer. Hepatology 2002;35:1134–43.
[23] Yamashita T, Honda M, Nakamoto Y, et al. Discrete nature of EpCAM+ and CD90+ cancer stem cells in human hepatocellular carcinoma. Hepatology 2013;57:1484–97.
[24] Wang X. Improving microRNA target prediction by modeling with unambiguously identified microRNA-target pairs from CLIP-ligation studies. Bioinformatics 2016;32:1316–22.
[25] Wong N, Wang X. miRDB: an online resource for microRNA target prediction and functional annotations. Nucleic Acids Res 2015;43:D146–52.
[26] Dweep H, Gretz N. miRWalk2.0: a comprehensive atlas of microRNA-target interactions. Nat Methods 2015;12:697.
[27] Dweep H, Sticht C, Pandey P, Gretz N. miRWalk–database: prediction of possible miRNA binding sites by "walking" the genes of three genomes. J Biomed Inform 2011;44:839–47.
[28] Paraskevopoulou MD, Georgakilas G, Kostoulas N, Vlachos IS, Vergoulis T, Reczko M, et al. DIANA-microT web server v5.0: service integration into miRNA functional analysis workflows. Nucleic Acids Res 2013;41:W169–73.
[29] Reczko M, Maragkakis M, Alexiou P, Grosse I, Hatzigeorgiou AG. Functional microRNA targets in protein coding sequences. Bioinformatics 2012;28:771–6.
[30] Agarwal V, Bell GW, Nam JW, Bartel DP. Predicting effective microRNA target sites in mammalian mRNAs. Elife 2015:4.
[31] Elmore S. Apoptosis: a review of programmed cell death. Toxicol Pathol 2007;35:495–516.
[32] Ouyang L, Shi Z, Zhao S, Wang FT, Zhou TT, Liu B, et al. Programmed cell death pathways in cancer: a review of apoptosis, autophagy and programmed necrosis. Cell Prolif 2012;45:487–98.
[33] Hanahan D, Weinberg RA. Hallmarks of cancer: the next generation. Cell 2011;144:646–74.
[34] Cory S, Adams JM. The Bcl2 family: regulators of the cellular life-or-death switch. Nat Rev Cancer 2002;2:647–56.
[35] Opferman JT, Korsmeyer SJ. Apoptosis in the development and maintenance of the immune system. Nat Immunol 2003;4:410–5.
[36] Tsujimoto Y, Ikegaki N, Croce CM. Characterization of the protein product of bcl-2, the gene involved in human follicular lymphoma. Oncogene 1987;2:3–7.
[37] Lin YC, Lin JF, Tsai TF, Chou KY, Chen HE, Hwang TI. Tumor suppressor miRNA-204-5p promotes apoptosis by targeting BCL2 in prostate cancer cells. Asian J Surg 2017;40:396–406.
[38] Renner W, Langsenlehner U, Krenn-Pilko S, Eder P, Langsenlehner T. BCL2 genotypes and prostate cancer survival. Strahlenther Onkol 2017;193:466–71.
[39] Eom YH, Kim HS, Lee A, Song BJ, Chae BJ. BCL2 as a subtype-specific prognostic marker for breast cancer. J Breast Cancer 2016;19:252–60.
[40] Callagy GM, Webber MJ, Pharoah PD, Caldas C. Meta-analysis confirms BCL2 is an independent prognostic marker in breast cancer. BMC Cancer 2008;8:153.
[41] Oltersdorf T, Elmore SW, Shoemaker AR, Armstrong RC, Augeri DJ, Belli BA, et al. An inhibitor of Bcl-2 family proteins induces regression of solid tumours. Nature 2005;435:677–81.
[42] Souers AJ, Leverson JD, Boghaert ER, Ackler SL, Catron ND, Chen J, et al. ABT-199, a potent and selective BCL-2 inhibitor, achieves antitumor activity while sparing platelets. Nat Med 2013;19:202–8.
[43] Han B, Park D, Li R, Xie M, Owonikoko TK, Zhang G, et al. Small-molecule Bcl2 BH4 antagonist for lung cancer therapy. Cancer Cell 2015;27:852–63.
[44] Chen G, Deng X. Targeting Bcl2 in cancer. Oncoscience 2015;2:813–4.
[45] Bartel DP. MicroRNAs: genomics, biogenesis, mechanism, and function. Cell 2004;116:281–97.
[46] Calin GA, Sevignani C, Dumitru CD, Hyslop T, Noch E, Yendamuri S, et al. Human microRNA genes are frequently located at fragile sites and genomic regions involved in cancers. Proc Natl Acad Sci U S A 2004;101:2999–3004.
[47] Wang Y, Li LJ, Qiu MX, Gong BS. Effects of paclitaxel combined with miR-448 on growth and proliferation of bladder cancer EJ cells. Europ Rev Med Pharmacol Sci 2018;22:3363–9.
[48] Zhu H, Zhou X, Ma C, Chang H, Li H, Liu F, et al. Low expression of miR-448 induces EMT and promotes invasion by regulating ROCK2 in hepatocellular carcinoma. Cell Physiol Biochem 2015;36:487–98.